

INFLUENCES OF FLUID PROPERTIES ON HEAT TRANSFER AND PRESSURE LOSS CHARACTERISTICS OF VISCOELASTIC FLUID FLOW IN SERPENTINE CHANNEL

Kazuya Tatsumi ***, Wataru Nagasaka*, Katsuki Kanaiwa and Kazuyoshi Nakabe ***

* Kyoto University, Kyoto 615-8530, Japan

** Advanced Research Institute of Fluid Science and Engineering, Kyoto University, Kyoto 615-8530, Japan

E-mail : tatsumi@me.kyoto-u.ac.jp

ABSTRACT

Heat transfer coefficient and pressure loss measurements and flow visualization were carried out for viscoelastic fluid flow in a serpentine channel. Water solutions of polyacrylamide (PAAm) and surfactant (CTAC) were used as viscoelastic fluids, and were compared with the Newtonian fluid case which was a sucrose solution. The visualized flow patterns showed that in the viscoelastic fluid case, unsteady flows with longitudinal vortices were generated in the serpentine channel even at $Re < 2.0$. A marked enhancement of heat transfer compared to the Newtonian fluid was obtained in this case. Further, the influences of the sucrose concentration of the viscoelastic fluids on the heat transfer and pressure loss characteristics were discussed. The results showed that a good correlation can be observed between the mean Nusselt number with the Weissenberg number than the Reynolds number in the case of PAAm solution. However, this correlation was not observed in the case of CTAC solution, the sucrose concentration of which was changed as the PAAm solution.

Keywords : Viscoelastic fluids, Heat transfer enhancement, Laminar flow, Serpentine channel

1. INTRODUCTION

It is known that viscoelastic fluids such as polymer solutions provide remarkable flow characteristics compared to Newtonian fluids. For example, application of shear stress to the viscoelastic fluid produces normal stresses which enhance the flow instability and generation of secondary flows. These flows can enhance fluid mixing and heat transfer compared with Newtonian fluids. Hartnett et al.[1] investigated laminar heat transfer characteristics of the viscoelastic fluid in a straight channel at $Re \sim 1000$ and showed that larger heat transfer coefficient can be observed in the viscoelastic fluid case which is believed to be attributed to the generation of secondary flows due to the normal stress differences. Groisman et al. [2] and Tamano et al. [3] have shown that strong unsteady and secondary flows are generated even under low Reynolds number conditions for viscoelastic fluid flows in serpentine channels. Recently, Zilz et al. [4] have carried out numerical and experimental investigation of the purely elastic flow instability in the serpentine channel. They have shown that the instability is mainly attributed to the curvature of the streamlines.

Higher heat transfer coefficient may be obtained in this case compared with the case of straight channel. However, heat transfer characteristics of such flows have not been studied yet. Therefore, in this study, heat transfer coefficient and pressure loss measurements were carried out for viscoelastic fluid flows in the serpentine channel under low Reynolds number condition ($Re \sim 1$). In addition to this, influences of the sucrose concentration of the viscoelastic fluid on the flow and heat transfer characteristics were measured. Furthermore, measurement was made for the heat transfer characteristics using surfactant solution (cetyltrimethylammonium chloride, CTAC) to see if the correlations using the present

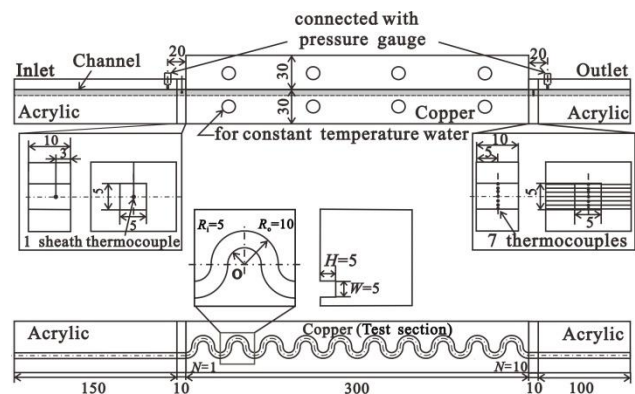


Fig.1 Apparatus and channel dimension used for heat transfer experiment.

non-dimensional values can be applied to different viscoelastic fluids.

2. EXPERIMENT

Two channels of different shapes are used in the experiment. One is a serpentine channel and the other is a straight channel. Figure 1 shows the schematic diagram and dimensions of the serpentine channel. The channel has a square cross section of 5×5 mm, and consists of semi-circular parts connected periodically in the streamwise direction. The inner and outer radii of the semi-circular part are $R_i=5$ mm and $R_o=10$ mm, respectively. The length along the serpentine channel, L , is 470 mm. The straight channel was designed to have the same channel length of 470 mm. Water of constant temperature was supplied to the copper block of the test section to heat the channel wall isothermally. Working fluid was supplied from the pressurized tank to the channel, and the mass of the fluid flowing from the outlet was measured by an electric weighing machine

Table. 1 Properties of the solutions (20°C, $\dot{\gamma}=50s^{-1}$).

Title	PAAm [wt%]	Sucrose [wt%]	μ [Pa · s]	λ [s]	Pr
Sucrose	-	64.4	0.15	-	1030
PAAm(64)	500	64.4	0.37	4.0	2340
PAAm(60)	500	60.0	0.16	3.5	1030
PAAm(57)	500	57.0	0.09	2.5	650

Table. 2 Properties of the solutions (20°C, $\dot{\gamma}=50s^{-1}$).

Title	CTAC [wt%]	Sucros e [wt%]	μ [Pa · s]	λ [s]	Pr
CTAC(64)	1000	64.4	0.37	4.0	2340
CTAC(60)	500	60.0	0.16	3.5	1030
CTAC(57)	200	57.0	0.09	2.5	650

Table. 3 Experimental condition (PAAm solution).

solution	Re	Gz	Wi	N_D
Sucrose	0.7-2.5	4-34	-	0.2-2.2
PAAm(64)	0.2-2.6	3-40	11-137	0.1-1.5
PAAm(60)	0.4-5.1	5-38	10-136	0.2-2.9
PAAm(57)	0.5-5.8	4-39	8-125	0.3-3.5

Table. 4 Experimental condition (CTAC solution).

solution	Re	Gz	Wi	N_D
CTAC(63)	1.3-3.7	6-22	45-180	0.8-2.2
CTAC (60)	0.9-5.1	4-30	35-190	0.5-3.0
CTAC (57)	0.8-7.5	4-49	35-250	0.5-4.2

to measure the mass flow rate, \dot{m} . The bulk mean temperatures of the fluid at the inlet and outlet of the test section ($T_{b,i}$, $T_{b,o}$) were obtained from the fluid temperature measured at each location and the fully developed velocity profile of a square channel. Single sheath thermocouple was used to measure the inlet fluid temperature while the outlet fluid temperature was measured by seven thermocouples located evenly in the height direction at the center of the channel width. The wall temperature, T_w , was a value of averaging the temperatures measured at seven locations of the copper block surface. Average heat transfer coefficient, h_m was thus calculated by applying the bulk mean temperature and mass flow rate to Eq. (1).

$$h_m = \frac{\dot{m}c_p}{A_s} \times \ln \frac{T_w - T_{b,i}}{T_w - T_{b,o}} \quad (1)$$

A_s is heat transfer surface area, \dot{m} is mass flow rate, and c_p is the constant pressure specific heat capacity. The average Nusselt number was defined as $Nu_m = h_m D_h / k$ where D_h is the hydraulic diameter of the channel, and k is the thermal conductivity.

Pressure loss, ΔP , was measured by two pressure gauges attached to the inlet and outlet of the test section as shown in Fig. 1. Visualization experiment was carried out for a serpentine channel made of transparent acrylic capturing the streakline

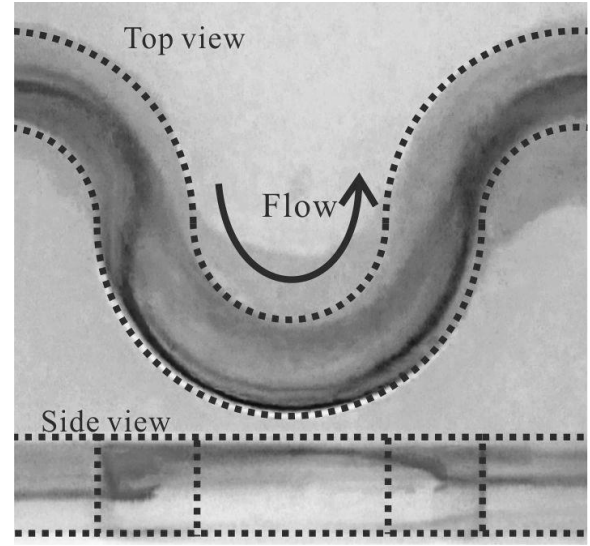


Fig.2 Flow visualized from side and top of the channel. (PAAm solution case).

images of dye using two video cameras. To supply the dye to the channel, a 1mm diameter tube with a pore pierced at the end was inserted perpendicular to the cross-section at the upstream of the channel. The dye was injected from the pore to the channel by a syringe pump at flow rate of 1mL/min.

An aqueous solution of 500ppm polyacrylamide (PAAm, $M_w=1.8 \times 10^7$), 1wt% NaCl, and sucrose was used as viscoelastic fluid. Sucrose was mixed in the fluid to modify the relaxation time of solution, while NaCl was added to prevent the aggregation of the polymers. Sucrose concentration was changed for three conditions, which are 57.0, 60.0 and 64.4 wt%, in order to evaluate the influence of the fluid property. In addition to this, surfactant (CTAC, cetyltrimethyl ammonium chloride: $M_w=320$) solution was investigated in this study. NaSal ($M_w=160$) sucrose were mixed as counter ion and to change the viscosity of the solution. Measurement of an aqueous solution of 64.4wt% sucrose was carried out as Newtonian fluid case to compare with the viscoelastic fluids case.

The viscosity μ and relaxation time λ are measured by a rheometer (ANTON PAAR, MCR301). The apparent viscosity of PAAm solutions is a function of shear rate and temperature. The relation of logarithm law shown in Eq. (2) is employed in this study.

$$\log_{10} \mu(T_m) = \alpha_\mu + \frac{\beta}{(T_m + 273)} + \frac{\varepsilon}{(T_m + 273)^2} \quad (2)$$

In this case, coefficients β and ε did not vary much in relation to the temperature and are kept constant as $\beta = -3.1 \times 10^3$ and $\varepsilon = 8.0 \times 10^5$. As for α_μ , the relationship with the shear rate is expressed by using the power law, $\mu = K\dot{\gamma}^{n-1}$. $\dot{\gamma}$ is the flow shear rate, n is constant, and K is a coefficient related to the temperature[5]. K and n are obtained for temperature of 20°C and shear rate $\dot{\gamma} = 1 \sim 100s^{-1}$ using the working fluid of each experiment.

α_μ can be calculated from Eq. (2). Then, μ of the reference temperature of the fluid of which the experiment was carried out is obtained. One example of K and n obtained from the PAAm

solution of the experiment are $K = 0.55$ and $n = 0.88$.

Since the PAAm concentration of the solution used in this study is small, a reliable measurement of the the relaxation time λ using the rheometer directly was difficult. Therefore, the Maxwell law of the stress relaxation is applied to the stress distribution after a constant strain is applied to the fluid. Measurement is carried out for the fluid temperature of 15, 20, 30 and 40 °C in order to obtain the relation based on Eq. (2).

Tables 1 and 2 summarize the values of μ , λ , and Prandtl number, $Pr = c_p \mu / k$ of the PAAm and CTAC solutions, respectively. These values are the results of the measurement at 20 °C and $\dot{\gamma} = 50 \text{ s}^{-1}$. c_p , k , and the density ρ of the solutions are referred to the values measured by Frank, T. [6] and Werner, M. [7]. Logarithmic mean temperature of $T_{b,i}$ and $T_{b,o}$ is used as reference temperature of the fluid in heat transfer measurement. Tables 3 and 4 show the non-dimensional values of the each solution. The Reynolds number, $Re = \rho U_m D_h / \mu$, was varied from 0.2 to 7.5. The Graetz number, $Gz = Re Pr D_h / L$, and Weissenberg number, $Wi = 4 U_m \lambda / D_h$, and Dean number, $N_D = Re \sqrt{D_h} / (R_i + R_o)$, corresponding to the Re condition.

3. RESULTS AND DISCUSSION

3.1 Visualization experiment

Figure 2 shows the result of the visualization for the flow of PAAm solution in the serpentine channel at $Re = 2.0$ ($Wi = 160$ and $ND = 1.2$). The result shows that the spanwise and height positions of the streaklines change as the fluid flows along the curve of the serpentine channel and that secondary flows are generated in the channel. Further, although not shown here, fluctuations of the streaklines were observed indicating the existence of unsteady flows. Particularly, in the area adjacent to the inflection points of the curved channel, the generation of longitudinal vortices was observed which accompanied a strong fluctuation of the streaklines. On the other hand, no fluctuations and secondary flows were observed in the sucrose solution case under all Re conditions tested in this study. Thus, the flow characteristics observed in the PAAm solution are attributed to the fluid viscoelasticity.

3.2 Heat transfer enhancement of the PAAm solution

Figure 3 shows the relationship between the Fanning's friction factor, $f = D_h \Delta P / 2 \rho U_m^2 L$, and modified Reynolds number, Re^* . Re^* is defined by Eq. (2).

$$Re^* = \frac{\rho U_m^{2-n} D_h^n}{8^{n-1} K (B + A/n)^n} \quad (2)$$

A and B are the geometrical constants. Figure 3 shows the friction factors of the PAAm(64) and the sucrose solutions in both case of the serpentine and straight channels. The theoretical values depicted in Figure 3 are the friction factors of steady flow in a square duct for Newtonian fluid [8] and non-Newtonian power-law fluid [9]. The influences of the temperature distribution appearing in the channel cross-section, and the dependency of the apparent fluid viscosity on the shear rate are taken into consideration for the theoretical values.

In both cases of the straight and the serpentine channels, f of

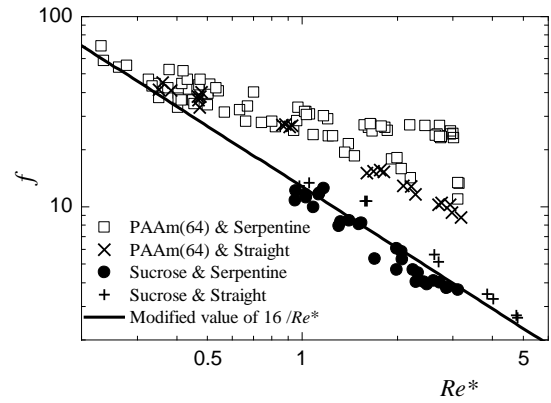


Fig.3 Relation between friction factor f and modified Reynolds number Re^* : comparison of serpentine and straight channels.

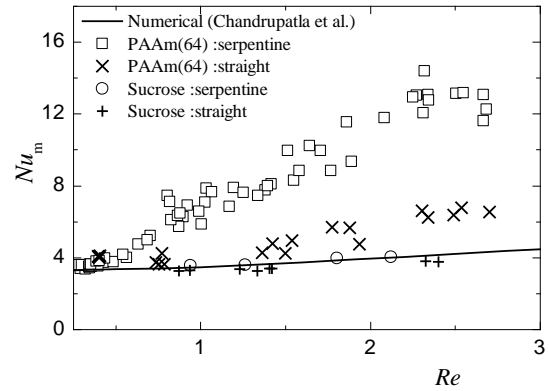


Fig.4 Relation between average Nusselt number Nu_m and Reynolds number Re : comparison of serpentine and straight.

the sucrose solution agrees well with the theoretical one. This result shows that the flow in sucrose solution case is steady and does not accompany any strong secondary flows even in the serpentine channel case. This is due to the small Dean number ($N_D \sim 1$) condition under which a Taylor-Dean flow was not generated. In the case of PAAm solution, the values of f of the experiment agree well with the theoretical ones for $Re^* < 0.4$. However, as Re^* increases, the experimental values are larger than the theoretical one. Therefore, a factor in addition to the shear thinning effect exists in the serpentine channel case, which is believed to be the transition of the flow from steady to unsteady state and the generation of secondary flows. Comparing the measurement results of the straight and serpentine channels, the value of the straight channel is smaller than that of the serpentine channel. The value is, however, larger than the theoretical one. Therefore, even in the straight channel case, secondary flows are generated which increases the pressure loss.

In Figure 3, an uncertainty of f is large for both cases of PAAm and sucrose solutions. This main reason is expected to be effects of temperature dependences of apparent viscosity. When the apparent viscosity of a working fluid largely changes depended on temperature, friction factor is different from a case of a constant temperature fluid. Therefore, the f values change

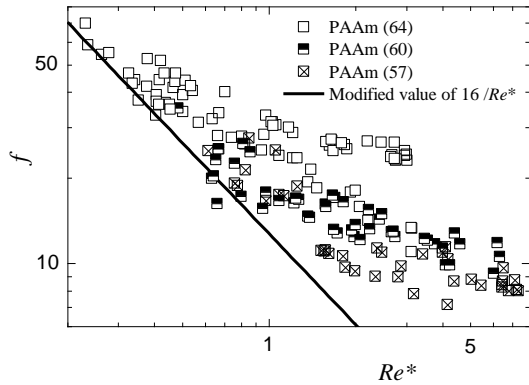


Fig.5 Relation between friction factor f and modified Reynolds number Re^* : comparison of PAAm(57)-(64).

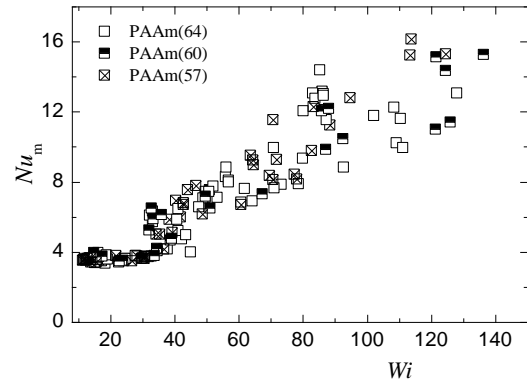


Fig.7 Relation between average Nusselt number Nu_m and Weissenberg number Wi in the serpentine channel: comparison of PAAm(57)-(64).

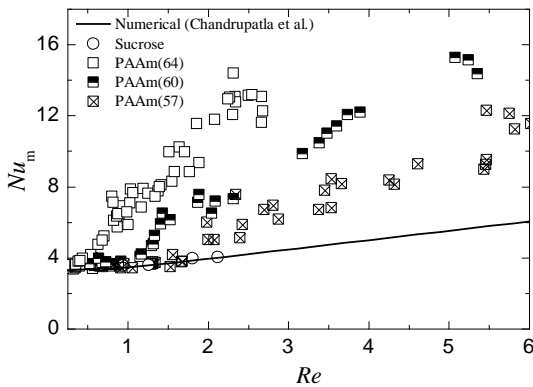


Fig.6 Relation between average Nusselt number Nu_m and Reynolds number Re in the serpentine channel: comparison of PAAm(57)-(64).

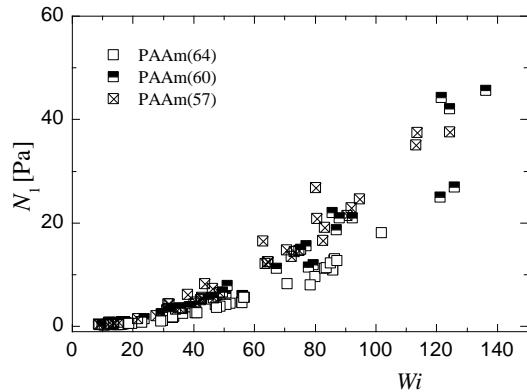


Fig.8 Relation between normal stress difference N_1 and Weissenberg number Wi : comparison of PAAm(57)-(64).

depended on the inlet temperature which decided by room temperature because a magnitude of the effects depends on differences between the wall temperature and the bulk temperature. Since experiments were carried out under various inlet temperatures of the range from 18°C to 23°C, the uncertainty of f in the Figure 2 is large.

Figure 4 shows the relationship between the average Nusselt number and Reynolds number. Both values of the serpentine and straight channels are shown in the figure. The numerical values shown in Figure 3 are the Nusselt number of steady Newtonian fluid flow in a square duct of which the developing region of the thermal boundary layer is considered [10]. The effects of the temperature dependence of the fluid viscosity are considered.

As Re increases, Nu_m of the sucrose solution slightly increases due to the influence of the entrance region of the thermal boundary layer. The result agrees excellently well with the numerical values showing the validity of the present measurement. In the case of sucrose solution, Nu_m of the serpentine channel shows a same value with the straight channel. This is because the present flow is in steady state, and moreover, the Dean number of the flow is small and no marked secondary flow is generated. The values of PAAm solution in the serpentine channel agree with the numerical one of the Newtonian fluid at $Re < 0.4$. However, as Re increases, Nu_m of PAAm solution

increases markedly and shows higher value compared with the case of Newtonian fluid. This result shows that heat transfer can be enhanced markedly by using the viscoelastic fluid and serpentine channel.

In the case of straight channel, Nu_m of PAAm solution increases as Re increases, and takes a greater value than the numerical results indicating heat transfer enhancement compared with Newtonian fluid. However, the values are smaller than the case of serpentine channel. Secondary flow is generated in the straight channel due to the square cross-section and the viscoelasticity of the fluid as mentioned in Section 1, and the heat transfer in the channel is enhanced. The flow in the straight and serpentine channels, however are believed to be different structure. The curve parts and inflection points in the serpentine channel influence the flow. These results show that the serpentine channel is needed to generate high heat transfer enhancement of viscoelastic fluid flow.

3.3 Influence of sucrose concentration of the PAAm solution

Figures 5 and 6 show the influences of the sucrose concentration of the PAAm solution on the relationship between f and Re^* , and between Nu_m and Re in the case of serpentine channel. As Re^* increases, the values of f increase in all cases

and show a larger value than the theoretical ones. However, since the viscosity and the relaxation time differs among the solutions with different sucrose concentrations, the Nu_m distributions shows a different tendency against Re . Namely, Nu_m of the three PAAm solutions increase markedly compared to numerical values. However the Reynolds number at which Nu_m starts to increase changes depending on the sucrose concentration. The distribution, therefore, cannot be correlated by the Reynolds number only, which implies that the flow and heat transfer characteristics of the PAAm solution relies on other physical properties of the viscoelastic fluid.

Figure 7 shows the relation of Weissenberg number Wi and Nu_m . One can see that a good agreement is observed among the three cases. Weissenberg number is known to represent the influence of the fluid viscoelasticity on the flow characteristics, particularly the normal stress differences. In order to see the influence of the first normal stress differences $N_1 = \tau_{11} - \tau_{22}$ on the heat transfer characteristics, Figure 7 shows the relation between Wi and N_1 , which is the value measured by the rheometer for each PAAm solution. In Figure 8, N_1 starts to increase at $Wi \sim 20$ which is a value close to the one at which Nu_m starts to increase. Further, N_1 of the PAAm (64), (60) and (54) solutions agree well with each other particularly in the area of $Wi < 60$. These results show that Wi has a correlation with N_1 , and that the normal stress which increases as Wi increases is one of the main reasons for the secondary flow generation and triggering the unsteady flow.

As Wi increases, a variation of Nu_m is observed in Figure 7. The reason for this is considered to be threefold. The first one is the variation of N_1 which becomes significant as Wi increases as shown in Figure 8. The second reason can be the influences of the increase of the Reynolds number and Dean number. As Re increases, the viscous dissipation decreases and the vortices generated at the inflection point in the channel are convected downstream. Under such situation, the dominant factor to present the flow structure in the serpentine channel might not only be the normal stress, i.e. Weissenberg number. The third reason can be related to the fact that the flow of the present study is in the region where the viscoelastic fluid flow transits from steady to unsteady flow. In such region, the flow can easily transit by any small disturbance such as the difference of inlet temperature. This region makes it difficult to carry out accurate measurements. The condition for generation of vortices is decided by Weissenberg number but the following flow is complicated and difficult to discuss heat transfer characteristics only by dimensionless number.

3.4 Heat transfer performance of the CTAC solution

Figure 9 shows the relationship between Nu_m and Re in the case of CTAC solutions. Nu_m shows a greater value compared with sucrose solution case over the range of Re considered here. Heat transfer enhancement is, therefore, achieved in the CTAC solution. Comparing Nu_m of PAAm and CTAC solutions, one can see that the influence of Re on Nu_m is relatively small and remains nearly constant in the CTAC solution case. Therefore, larger Nu_m is obtained in the CTAC case for smaller Re conditions, and as Re increases, Nu_m of PAAm solution case

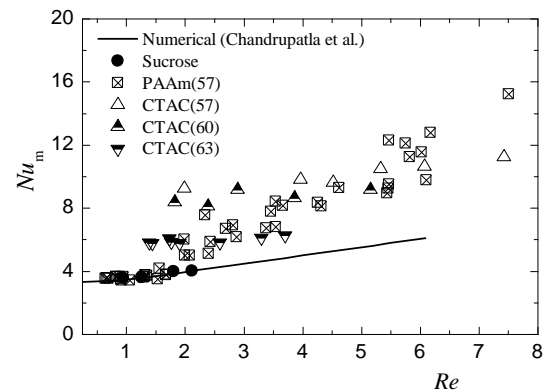


Fig.9 Relation between average Nusselt number Nu_m and Reynolds number Re in the CTAC solution case.

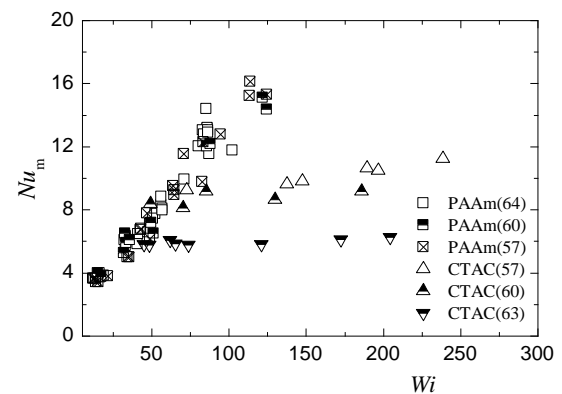


Fig.10 Relation between average Nusselt number Nu_m and Weissenberg number Wi in the CTAC solution case.

becomes larger than that of the CTAC case.

Comparing the Nu_m of the CTAC solutions with different sucrose concentrations (57), (60) and (63), CTAC solution with higher sucrose concentration shows larger Nu_m . In any case, a good correlation cannot be found between the Re and Nu_m .

Figure 10 shows the relationship between Wi and Nu_m . As was found in Fig. 7, Nu_m increased with Wi in the case of PAAm solution. However, in the case of CTAC solution, Nu_m remains constant. Furthermore, different distributions are observed for different sucrose concentration in the case of CTAC solution indicating that Wi may not be the effective to represent the flow and heat transfer characteristics of the CTAC solution in the serpentine channel.

One reason may be the difference in the relaxation time. Greater value is obtained in the CTAC solution compared with the PAAm solution as shown in Tables 1 and 2. Considering the flow velocity and the periodical structure of the serpentine channel, the influence presented by the Deborah number can become more conspicuous in the CTAC solution case. Another can be the influence of the entrance region effect. In the present heat transfer measurement includes a long range of the entrance region. If this region shows a dominant effect on the heat transfer performance, and if the Wi characterizes more of the heat transfer performance in that area, then the CTAC solution, the flow of which could be fully developed in a shorter length, may not be represented by Wi . Further discussion is needed as future

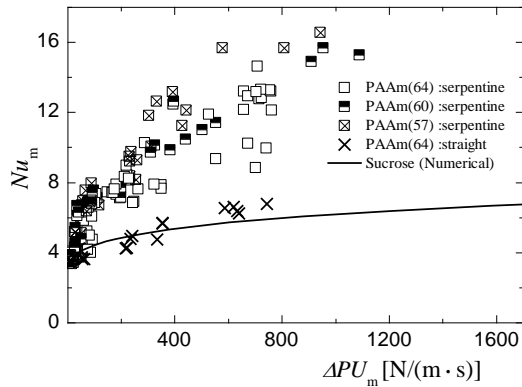


Fig.11 Relation between average Nusselt number Nu_m and pumping power.

work for this problem.

3.5 Pumping power

Figure 11 shows the relation between Nu_m and pumping power ΔPU_m . The values of Nu_m of PAAm solutions in the case of serpentine channel is larger than those of the sucrose solution particularly in the range of $\Delta PU_m > 100$. In the case of PAAm solution in the straight channel, the values are almost the same as the sucrose solution. Thus, even if the pressure loss increases due to the fluctuations and secondary flows, PAAm solution in the serpentine channel under the conditions of high viscosity and low Reynolds number shows the highest overall performance.

In Figure 8, comparing Nu_m of the three PAAm solutions, the case of PAAm (57) shows the largest value in the area of $\Delta PU_m > 300$ indicating that the solution of smaller sucrose concentration shows higher overall performance. The reason for this is considered to be as follows. As shown in Figure 7, N_1 takes larger value in the order of PAAm (57), (60), and (64) for the same Wi . Thus, largest Nu_m is observed in the case of PAAm (57) in Figure 6. In addition to this, as shown in Table 1, the fluid viscosity μ decreases significantly as the sucrose concentration decreases, while the difference of the relaxation time λ is relatively small. Therefore, when considering identical Wi condition, a similar or larger Nu_m can be obtained in the PAAm (57) case for the same U_m . Obviously, smaller pumping power is required for PAAm (57) case since μ is considerably small compared to other PAAm solutions.

4. CONCLUSIONS

The heat transfer and pressure loss characteristics of viscoelastic fluid in the serpentine channel was experimentally investigated. The average Nusselt number Nu_m increased in the case of viscoelastic fluid (PAAm solution) in the serpentine channel compared with the cases of PAAm solution in the straight channel and sucrose solution (Newtonian fluid). The highest overall performance considering the pumping power was observed in the case of viscoelastic fluid flow in serpentine channel. When the sucrose concentration of the PAAm solution was changed, a poor correlation was observed between the Reynolds number and Nu_m . On the other hand, a good

correlation was obtained by using the Weissenberg number. However, in the case of CTAC solution, Nu_m could not be characterized by Wi . The present experimental results showed that as Weissenberg number increases, several fluid properties would influence the flow field, thus, particularly Re , Pr and λ should be taken into consideration to describe the heat transfer characteristics.

ACKNOWLEDGEMENT

This work was supported by Japan Society for the Promotion of Science (JSPS) KAKENHI Grant-in-Aid for Scientific Research(B), grant Number 24360080.

REFERENCES

- Hartnett, J. P. and Kostic, M., Heat Transfer to a Viscoelastic Fluid in Laminar Flow through a Rectangular Channel, *Int. J. Heat Mass Transfer*, vol. 28, no. 6, pp. 1147-1155, 1985.
- Groisman, A. and Steinberg, V., Efficient Mixing at Low Reynolds Numbers Using Polymer Additives, *Nature*, vol. 410, pp. 905-908, 2001.
- Tamano, S., Itoh, M., Sasakawa, A. and Yokota, K., PIV Measurement of Secondary Flow in Curvilinear Pipe Flow of Polymer Solution, *Trans. JSME, Ser. B*, vol. 75, no. 759, pp. 2115-2121, 2009.
- Zilz, J., Poole, R.J., Alves, M.A., Bartolo, D., Levache, B. and Lindner, A., Geometric Scaling of a Purely Elastic Flow Instability in Serpentine Channels, *J. Fluid Mech.* vol. 712, no. 712, pp. 203-218, 2012.
- Mirsa, B. N. and Varshni, Y. P., Viscosity-Temperature Relation for Solution, *J. Chem. Eng. Data*, vol. 6, no. 2, pp. 194-196, 1961.
- Frank, T., Gucker, Jr. and Fred, D. A., The Specific Heat of Aqueous Sucrose Solutions at 20°C and 25°C and the Apparent Molal Heat Capacity of Non-Electrolytes, *J. American Chem. Society*, vol. 59, no. 3, pp. 447-452, 1937.
- Werner, M., Baars, A., Werner, F., Eder, C. and Delgado, A., Thermal Conductivity of Aqueous Sugar Solutions Under High Pressure, *Int. J. Thermophysics*, vol. 28, pp. 1161-1180, 2007.
- Kays, W. N. and Crawford, M. E., *Convective Heat and Mass Transfer, Second Edition*, McGraw-Hill, pp. 275-287, 1980.
- Kozicki, W., Chou, C. H. and Tiu, C., Non-Newtonian Flow in Ducts of Arbitrary Cross-Sectional Shape, *Chemical Engineering Science*, vol. 21, pp. 665-679, 1966.
- Chandrupatla, A. R. and Sastri, V. M. K., Laminar Forced Convection Heat Transfer of a Non-Newtonian Fluid in a Square Duct, *Int. J. Heat Mass Transfer*, vol. 20, pp. 1315-1324, 1977.